Reconfigurable Assemblies of Shape-Changing Nanorods

Trung Dac Nguyen[†] and Sharon C. Glotzer[†,‡,*]

[†]Department of Chemical Engineering and [‡]Department of Materials Science and Engineering, University of Michigan, Ann Arbor, Michigan 48109

I t is well-known that certain organic supramolecules and liquid crystals exhibit conformational changes under external stimuli such as temperature, pressure, stress, solution pH, and electric or magnetic fields.[1-10] Such microscopic changes can lead to macroscopic structural transformations which, in turn, result in significant variation in materials' properties such as elastic modulus, thermal conductivity, bioactivity, and electromagnetic resonance.[4-6] For example, Kim *et al.* reported thermally responsive capsule structures with 25 nm diameter pores in a shell formed by the hierarchical self-assembly of double tethered rod amphiphiles.[7] The hydrophilic oligo(ethylene oxide) coils at one end of the rods shrink upon heating or expand upon cooling, resulting in a reversible closed/open gating motion of the nanopores. Recently, Lee *et al.* further demonstrated a reversible transformation between two-dimensional sheets and tubular structures assembled by laterally grafted rod amphiphiles, also upon heating.[9] These transformations, however, are not between equilibrium states but are instead strongly pathway-dependent, and thus the resulting structures depend on the initial state of the material. The resulting structures, therefore, may become trapped in local energy minima and are stable under thermal fluctuations. Taking advantage of these kinetic effects, various experimental studies have progressed in engineering higher-order structures that are inaccessible under self-assembly from isotropic states. Ciszek *et al.* demonstrated that two-dimensional flat sheets assembled by amphiphilic rod-like peptides on a template fold into hollow spheres whose structure depends on the initial sheet pattern.[10] Upon drying, the polymer tethers attached to

one end of the rods contract, forcing the flat sheet to curve to reduce the exposure of its hydrophobic surfaces. Our previous simulations predict that flat bilayer sheets of P_2 symmetry assembled by laterally tethered rod-like nanoparticles and their molecular analogues[11,12] scroll into distinct helical structures, which can transform from one morphology to another by switching the selective solvent conditions.[13] Switching the solvent condition changes the rod−rod and tether−tether interactions, allowing the sheet to fold or unfold reversibly in most cases. In those studies, solvophobic forces guide the system toward a certain target structure. However, since the resulting structures are not necessarily at equilibrium, the assembly pathway is unreliable relative to that between

ABSTRACT Reconfigurable nanostructures represent an exciting new direction for materials. Applications of reversible transformations between nanostructures induced by molecular conformations under external fields can be found in a broad range of advanced technologies including smart materials, electromagnetic sensors, and drug delivery. With recent breakthroughs in synthesis and fabrication techniques, shape-changing nanoparticles are now possible. Such novel building blocks provide a conceptually new and exciting approach to self-assembly and phase transformations by providing tunable parameters fundamentally different from the usual thermodynamic parameters. Here we investigate *via* molecular simulation a transformation between two thermodynamically stable structures self-assembled by laterally tethered nanorods whose rod length is switched between two values. Building blocks with longer rods assemble into a square grid structure, while those with short rods form bilayer sheets with internal smectic A ordering at the same thermodynamic conditions. By shortening or lengthening the rods over a short time scale relative to the system equilibration time, we observe a transformation from the square grid structure into bilayer sheets, and *vice versa*. We also observe honeycomb grid and pentagonal grid structures for intermediate rod lengths. The reconfiguration between morphologically distinct nanostructures induced by dynamically switching the building block shape serves to motivate the fabrication of shape-changing nanoscale building blocks as a new approach to the self-assembly of reconfigurable materials.

KEYWORDS: reconfigurable materials' nanostructures · self-assembly · laterally tethered nanorods · computer simulation

equilibrium structures because it depends on kinetics and initial states.

Experiments, theories, and simulations reported in the literature have shown that for rod−coil molecules,[14−20] block copolymers,[21−23] and tethered nanoparticle shape amphiphiles[11,24−35] the volume fraction and geometry of the constituent components play key roles in the morphology of the assembled structures. For instance, depending on the volume fraction of rod and coil segments, rod−coil molecules in an aqueous medium form cubic ordered micelles, tetragonally or hexagonally packed columns, or lamellar structures.[15] In a solvent good for the tethers and poor for the rods, end-tethered rods assemble into hexagonally packed cylinders with a helical twist if the rod length is comparable to the tether extended length.[25,29] The helical twist is diminished if the rods are shorter than the tethers due to the entropic effects of the tethers.[29] In previous self-assembly simulations, transitions from isotropic states to ordered structures focus primarily on equilibrium structures. The systems are initially relaxed at high temperature or dilute concentration and then cooled or compressed gradually. At each temperature or pressure step, the systems are equilibrated until some order parameter, such as the system potential energy, becomes stable. The influences of volume fraction and shape anisotropy of the constituent components on the assembled structures are therefore usually studied by conducting independent simulations[11,18,23−34] or experiments[12,19,22] on different building blocks and molecules. Ryu and co-workers have reported various hierarchically assembled nanostructures based on rod−coil molecules with different topologies.[14,15] Numerous simulations on polymer-tethered nanoparticle building blocks[24] including spheres,[26,31,33] rods,[11,18,25,29] cubes,[27,28] and V-shaped nanoparticles,[32] and recently theoretical treatments,[35] have also emphasized the significance of shape anisotropy with regards to the phase behavior and local packing of shape amphiphiles.

However, there have been few studies on how a dynamic change in the building block geometry or conformation, particularly at nanometer length scales, would lead to predictable morphological transformations between assembled structures.[7,9,10,36−42] Polypeptide-based block copolymers, for example, were shown recently to be potential candidates for stimuli-responsive building blocks.[36−40] Gebhardt et al. demonstrated that the polypeptide rod segment in poly(butadiene)-poly(L-lysine) block copolymers undergoes a reversible conformational α-helix−coil transition in response to a change in pH and temperature.[39] Another recently demonstrated approach is to employ DNA strands as a reconfigurable linker between particles to toggle between different states of self-assembled structures.[41,42] For instance, Maye and co-workers showed that interparticle distances in superlattices and dimer clusters as-
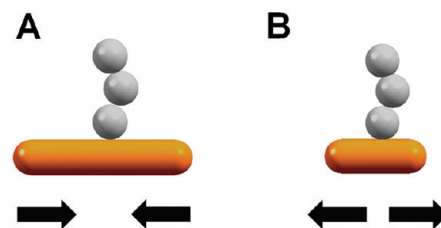

Figure 1. Laterally tethered nanorods with (A) a 5σ rod and (B) a 3σ rod studied computationally in this work. The rods, drawn as smooth, consist of five spherical beads with diameter σ placed at a center−center distance of σ for longer rods and 0.5σ for shorter ones. The tether consists of three spherical beads with diameter σ, unless otherwise noted. Rod beads are in yellow, tether beads are in white. Arrows indicate the directions of (A) shortening and (B) lengthening the rods.

sembled by gold nanoparticles with DNA linkers can be dynamically tuned by adding small "set" or "unset" DNA strands.[42] It has also been shown experimentally that colloidal gold nanorods can be shortened or morphed into other shapes such as spheres, bent rods, twisted rods or "ϕ" shapes by using laser pulses with different wavelengths and widths.[43−45] Given the variety of diverse nanocolloid shapes that is now possible,[46] fabricating particles from materials that allow a reversible shape change upon application of an external trigger, such as light, would create enormous possibilities for a new class of reconfigurable materials. Polymeric nanorods composed of an anisotropically cross-linked gel, for example, could be made to swell or contract lengthwise, lengthening and shortening the rod, respectively. Other more complex geometry changes may also be envisioned.

Here, using a generic coarse-grained bead−spring model of laterally tethered nanorods (Figure 1) interacting via empirical pair potentials, we investigate the spontaneous transformation between two equilibrium structures that each result from the self-assembly, at melt densities, of two types of laterally tethered nanorods that differ only in their rod length. Attractive interactions that lead to the aggregation of rods and of tethers are modeled by a Lennard-Jones potential with a short-range cutoff, and the immiscibility between rods and tethers is modeled by a purely repulsive Weeks−Chandler−Andersen potential. We find that the building blocks with longer rods assemble into a 3-D columnar square grid structure, while those with shorter rods form bilayer sheets at the same number density and reduced temperature. By shortening or lengthening the rods of the assembled structures quickly relative to the system re-equilibration time, we show that the square grid structure reconfigures rapidly to bilayer sheets, and vice versa. We show that kinetic effects do not prevent the system from evolving between these two structures in either direction, suggesting an experimentally viable approach to nanoparticle shape-induced reconfigurability in these systems. Ordered periodic structures like those we obtain have

been shown to be useful for a range of applications including, but not limited to, optical materials with, for example, a photonic band gap, or negative index of refraction,[15,20] or materials with anisotropic mechanical properties. From this model system of building blocks with switchable shape, we aim to inspire the fabrication of reconfigurable nanomaterials from laterally tethered nanorods and their analogues.

RESULTS AND DISCUSSION

We observe upon cooling at fixed volume fraction the formation of a square grid structure and bilayer sheets from the thermodynamic self-assembly of laterally tethered nanorods for longer and shorter rods, respectively. Our results are in good agreement with previously reported experiments on geometrically analogous rod−coil molecules, which observe both of these phases.[16,17] Since we ascertain that the simulated structures are equilibrium structures, this suggests the experimental structures are likewise thermodynamically stable. Starting from an equilibrium assembled structure (either square grid or bilayers), we shorten or lengthen the rods, respectively, to the target length and monitor the morphological transformation to the other structure. We compare the time scale of the order−order transformation induced by rod shortening and lengthening with that of the self-assembly from isotropic states.

Self-Assembly of Longer Rods. At a number density of 0.8, we observe that laterally tethered nanorods in which the rod has a length of 5.0σ undergo a disorder−order transition from a disordered state to a 3-D square grid structure at $T \leq 2.2\varepsilon/k_B$ (Figure 2A,B). This morphology may also be called the tetragonal columnar phase because the tethers aggregate into columns, which are separated by a square grid of rods. Similar tetragonal morphologies have been observed computationally in systems of ditethered nanospheres[31,33] and experimentally with amphiphilic dumbbell-like and rod−coil molecules with a comparable aspect ratio of rod−coil segments; however, in the latter, the structure of the stacked rods between tether columns was not known.[16,17] The formation of columnar structures stems from the lateral constraint between the tether and the rigid part of the building block and their relative lengths according to a geometrical packing analysis.[21,26]

Simulation snapshots reveal how the rods arranged into a square grid pack into bilayer ribbons as the structure extends into the third dimension to maximize their contacts and offset randomly along the axial direction (Figure 2B) to mitigate the conformational entropy loss of the adjacent tethers. The structure can be characterized by the radial rod−rod correlation distribution $g_{R−R}(r)$ given in Figure 2C, in which the sharp first peak at 1.0σ indicates the side-by-side rod separation and the small second peak in the vicinity of 2.0σ shows
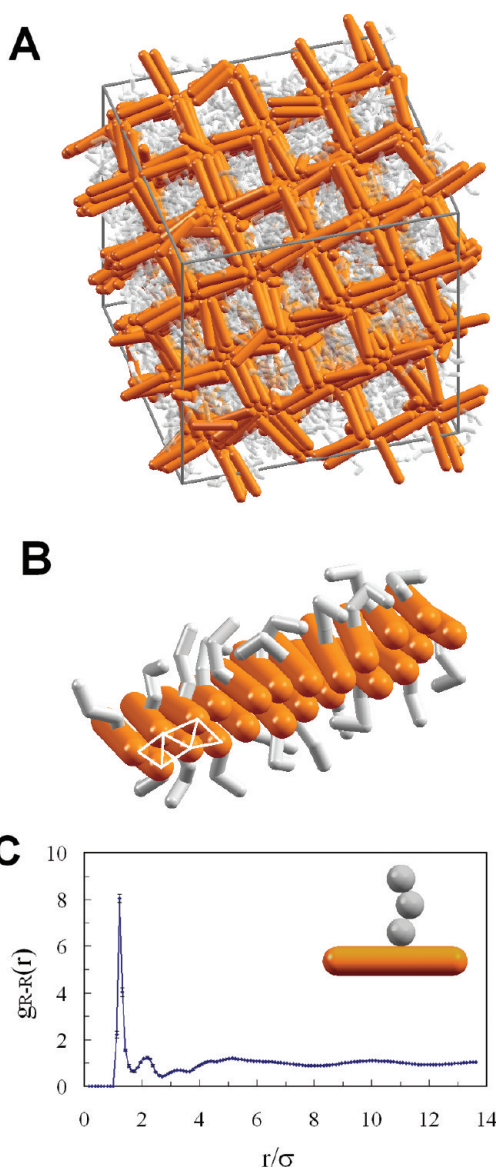

Figure 2. (A) Simulation snapshot of a columnar square grid structure formed by laterally tethered nanorods with a 5σ long rod. Rods are visualized as smooth for clarity of local packing of the rods. (B) Portion of a bilayer ribbon extracted from the structure shown in (A). (C) Radial rod−rod correlation function averaged over 10 snapshots taken every 1 million time steps. Error bars indicate the standard deviation from the average values.

the rod packing in linear bilayer ribbons. The two broad peaks at 5.0σ and 10.0σ represent the distances between parallel ribbons, respectively.

Self-Assembly of Shorter Rods. Laterally tethered nanorods for which the rod has a length of 3.0σ assemble into bilayer sheets for $T < 2.0\varepsilon/k_B$ at a number density of 0.8 (Figure 3A). Sheet-like (lamellar) structures have been shown to be thermodynamically stable for block copolymers and shape amphiphiles at a sufficiently high concentration and certain relative volume fractions of the immiscible constituents.[11,17] The formation of sheet-like structures again can be explained by a geometrical packing analysis based on the relative
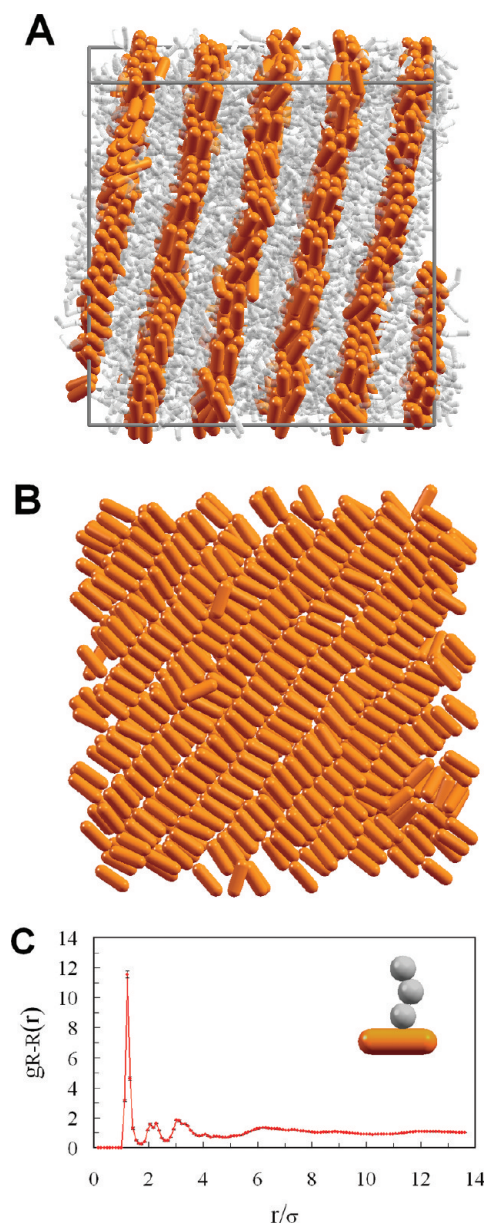
Figure 3. (A) Simulation snapshot of bilayer sheets formed by laterally tethered nanorods with a (short) 3σ rod. Rods are visualized as smooth for clarity of local packing of the rods. (B) Top view of a single bilayer sheet extracted from the structure shown in (A). The tethers are removed for clarity. (C) Radial rod−rod correlation function averaged over 10 snapshots taken every 1 million time steps. Error bars indicate the standard deviation from the average values.

lengths of the rods and the tethers.[11,21] By forming bilayer sheets, the rods maximize their contacts and allow the laterally attached tethers to maximize their free volume. Interestingly, when $T < 1.5\varepsilon/k_B$, the rods within each sheet arrange into smectic sublayers with P_2 symmetry due to stronger side-by-side, as compared to end-to-end, attractive interactions between rods (Figure 3B). The P_2 symmetry packing of the rods within bilayer sheets was predicted in previous simulations by Horsch et al. of a solution of laterally tethered solvophobic rods with the same rod−tether length ratio.[11] Recently, Hong and co-workers observed the formation of scrolled bilayer sheets with similar rod packing pattern in a solid melt of laterally grafted rod molecules.[12] We thus conclude that two key ingredients for the emergence of the rod bilayers and the crystalline P_2 symmetry packing within each bilayer are (i) the immiscibility between the rods and the tethers and (ii) the attraction between the rods. In our model, the attraction energy per unit rod length is greater in the shorter rod than in the longer rod with the same number of beads, compensating the entropy loss of tightly packed (but attractive) tethers, and allowing for an almost zero tilt angle of the rods within the smectic sublayers (i.e., smectic A ordering). The simulation snapshot (Figure 3A) further indicates that the average distance between adjacent bilayers is approximately twice the extended length of the tethers. Consequently, the coupling between adjacent bilayers is weak so that the sublayer axial directions in bilayers are uncorrelated. We also note that the cross section of the bilayers is similar to that of the ribbons in the columnar square grid structure (Figure 2B); this will play a role later when we examine the transformation between the two structures. The radial rod−rod correlation function in Figure 3C shows a sharp peak at a distance of 1.0σ indicative of the side-by-side rod packing, a split second peak at 2.0σ and 2.3σ characteristic of a crystalline packing of the rods in bilayers, and a third peak at 3.0σ corresponding to the distance between smectic sublayers.

Reconfigurability between Ordered Structures. For the purposes of comparing the self-assembly from initially disordered states of the ordered structures presented above with reconfiguration between the ordered structures, we define an assembled structure as a structure formed by cooling the system from disordered states and a transformed structure as one formed from a different ordered structure after the rods are lengthened or shortened rapidly. At temperature $T = 1.4\varepsilon/k_B$, which is below the disorder−order transition temperatures for both structures, we shorten and lengthen the rod both from assembled structures and from transformed structures to ascertain that the resulting structures are neither kinetically arrested nor metastable and that the transformation is reversible. The morphological evolution from the square grid structures to bilayer sheets and vice versa is monitored by the change in $g_{R-R}(r)$ and the system potential energy U. A transformation is considered complete if the fluctuations in these quantities are less than $5-10\%$. We found no significant difference in the final structures in terms of structural and energetic characteristics between starting from disordered states versus starting from a transformed structure, indicating that, like the assembled structures, the transformed structures are thermodynamically stable and at equilibrium.

Shortening Rods. Starting with the square grid structure formed by rods of length 5σ, we shorten the rods to 3σ over 10 000 time steps. As shown in Figure 4A (left),

the system potential energy drops from the value corresponding to the square grid structure, that is, $(4.67 \pm 0.01)\varepsilon$ per bead, to that corresponding to the bilayer sheets assembled from short rods, that is, $(3.57 \pm 0.01)\varepsilon$ per bead. Figure 4B (left) shows $g_{R\text{-}R}(r)$, which demonstrates that the transformation into bilayer sheets completes within ~20 million steps. After rod shortening, the square grid structure becomes unstable because the tether columns are no longer separated by the bilayer ribbons, and tethers in adjacent columns are free to interact with each other. The ribbons, however, remain due to the stronger side-by-side attractions between the rods as indicated by the first sharp peak in $g_{R\text{-}R}(r)$. The ribbons subsequently merge into larger sheets, becoming smectic sublayers within each sheet. In certain runs, we observe defects in the transformed bilayer sheets in which several smectic sublayers (previously ribbons) misalign with the rest (not shown), presumably due to imperfections in the starting structures.

Lengthening Rods. The rod segments are lengthened from 3σ to 5σ over 10 000 time steps starting with stable bilayer sheet structures. The long rods subsequently attempt to rearrange themselves to increase their contacts, leading to the corruption of the bilayer sheets. The system potential energy jumps to the value corresponding to the square grid structure obtained from self-assembly of long rods, that is, $(4.67 \pm 0.01)\varepsilon$ per bead. The transformation process completes after approximately 20 million steps as determined by the small fluctuations in U (Figure 4A, right) and $g_{R\text{-}R}(r)$ (Figure 4B, right). During equilibration, the split in the second peak and third peak of $g_{R\text{-}R}(r)$ vanishes, implying that the smectic sublayers no longer exist; however, the presence of the first sharp peak indicates that the side-by-side rod packing persists. The smaller value of $g_{R\text{-}R}(r)$ at the first peak indicates a lower probability of finding side-by-side neighbors and also suggests that the sheet-like aggregates of the rods disappear. We also note that the time evolution of $g_{R\text{-}R}(r)$ occurs in the reverse direction as compared to when the rods are shortened.

The driving force for the reconfiguration between the columnar square grid structure and bilayer sheet structure originates from the minimization of the system free energy, which involves the simultaneous maximization of energetically favored rod–rod and tether–tether contacts and conformational entropy of the flexible tethers. However, unlike self-assembly processes in which initial configurations are disordered, shape-changing induced transformation processes of the type studied here proceed from ordered states, which might suffer unfavorable kinetic effects hindering or preventing the formation of target structures. By shortening and lengthening the rods on a time scale much shorter than the system equilibration time, which is on the order of 40 million steps at $T = 1.4\varepsilon/k_B$ and $\Delta t = 0.002\tau$, we aim at reproducing experimental con-
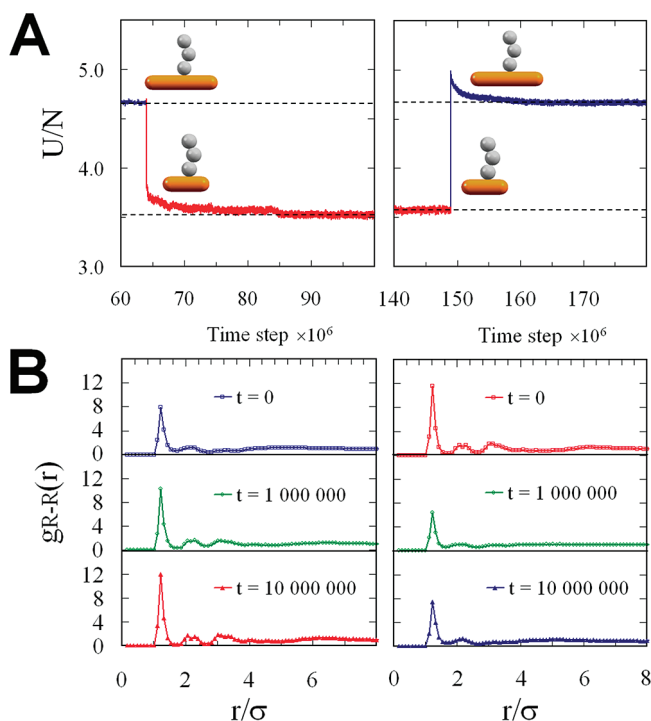

Figure 4. (A) Per bead potential energy and (B) radial rod–rod correlation functions during the transformation processes. The rod shortening and lengthening processes are illustrated by the images in the left and right columns, respectively.

ditions to examine if kinetic effects due to rod lengthening/shortening would prohibit the formation of target structures. In fact, with different shape-changing rates (*i.e.*, $2 \times 10^{-2}\sigma$, $2 \times 10^{-3}\sigma$, $2 \times 10^{-4}\sigma$, and $2 \times 10^{-5}\sigma$ every 10 time steps), the transformations all complete within the system relaxation time, and the system smoothly reconfigures to its new equilibrium, ordered state. Such a process is necessary for shape-induced transformation to be a reliable and predictable way to reconfigure materials' structures.

Intermediate Rod Lengths. Since a small change in the rod length gives rise to such a significant transformation in the symmetry of the structures, it is reasonable to investigate whether there may exist an intermediate rod length between 5σ and 3σ at which the system undergoes an order–order transition between structures with one- (in the case of sheets) and two- (in the case of grids) dimensional periodicity. We perform independent self-assembly simulations with intermediate rod lengths of 3.25σ, 3.375σ, 3.5σ, 3.75σ, and 4.0σ (Table 1 and Supporting Information). While rods of length 3.25σ assemble into bilayer sheets, rods of length 3.375σ, 3.5σ, 3.75σ, and 4.0σ form stretched honeycomb (not shown), honeycomb (Figure 5A), and pentagonal grids (Figure 5B), respectively. The critical rod length for the transition from a 1-D periodic (sheets) to 2-D periodic (stretched honeycomb grid) structure therefore falls inside a small window from 3.25σ to 3.375σ. It is interesting to note the sensitivity of the assembled structure to minute changes in the aspect ra-

TABLE 1. Assembled Structures Formed with Different Rod Lengths and the Dimensionality of the Periodicity of the Structures

rod length, σ	assembled structure	dimensionality of periodicity
3.0	bilayer sheets	1
3.25	bilayer sheets	1
3.375	stretched honeycomb grid	2
3.5	honeycomb grid	2
3.75	honeycomb grid	2
4.0	pentagonal grid	2
5.0	square grid	2

tio of the rods. More importantly, this sensitivity suggests the possibility of toggling between not just two but among multiple structures with only slight changes in rod length.

As predicted by theory and simulations and confirmed by experiments, the volume fraction of constituent components of rod−coil molecules,[14−20] block copolymers,[21−23] and shape amphiphiles[11,24−35] determines the assembled morphology at a given concentration. Consequently, one may argue that decreasing the rod length while keeping the tether length fixed is equivalent to keeping the rod length fixed while increasing the tether length, and *vice versa*. Although this
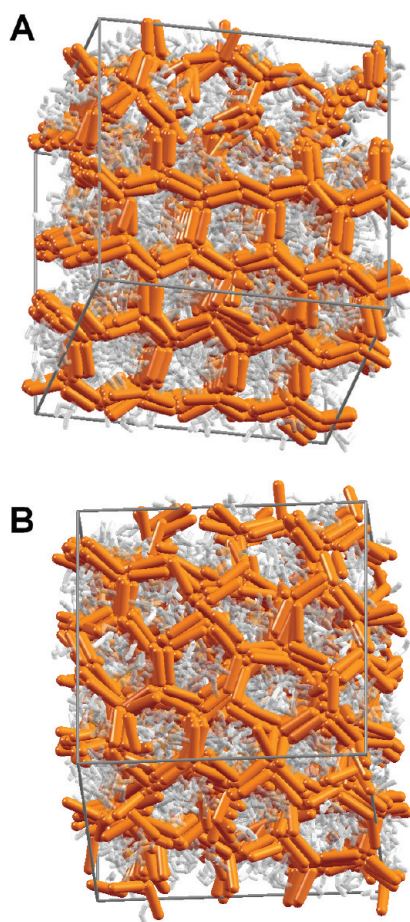

Figure 5. (A) Honeycomb grid structure formed by rods with a length of 3.5σ. (B) Pentagonal grid structure formed by rods with a length of 4.0σ.

may hold true for amphiphilic end-tethered rod systems, the anisotropic nature of the laterally tethered rods causes an asymmetric phase behavior with respect to the constituent volume fraction. While a small change in the rod length can lead to a significant morphological transition, a much larger variation in the tether length is required for such a transition. Simulations with a rod length of 5σ indicate that the tether length should be increased from 3σ to 10σ to induce a transformation from the columnar square grid structure to bilayer sheets. Moreover, since the increase in the tether length adds more mobility to the system, the disorder−order temperature is lowered, and thus the transformation may not occur at constant temperature as opposed to a small increase in the rod length. We attribute such asymmetric phase behavior to the building block anisotropy caused by the rigid rod segment. Since it is evident that the rods form bilayer ribbons in both structures, we argue that the rod length, which is related to the ribbon width, helps guide the aggregation of the ribbons while maximizing the entropy for the tethers. Meanwhile, the entropic effects of the flexible tethers on ribbon aggregation only become significant when the variation in the tether length is sufficiently large. For instance, additional simulations indicate that, for longer rods, the tether should be as much as three times longer, that is, consisting of 9 beads, to induce the formation of bilayer sheets. In their recent simulations of bola-amphiphilic liquid crystals with a lateral flexible chain, an analogue of our model laterally tethered rod, Crane and co-workers also showed that while the columnar phases form with a tether length of 3 beads, the lamellar phases only emerge when the chain length is greater than 11 beads.[18] It is therefore instructive that the responsiveness of laterally tethered rod systems to the rod length is greater than that to the tether length.

We note that, in addition to rod−tether relative volume fraction, other factors affect the formation of assembled and transformed structures, such as tether attachment point, tether flexibility, and particle shape. For example, if the point of tether attachment is moved from the rod center to an end, smectic structures will be expected to form.[34] It will be interesting to investigate in future studies how decreasing the tether flexibility or anisotropically deforming the rod shape (*e.g.*, into a cone-like shape) would lead to further novel structural transformations.

Time Scales for Self-Assembly *versus* Transformation. It is interesting to compare the dynamics of the transformation process to that of the self-assembly process starting from isotropic states to ascertain whether a given ordered structure forms more easily *via* transformation or self-assembly. To do this, in addition to $g_{R-R}(r)$ and U, we use the shape matching algorithms proposed by Keys *et al.*[47] to derive an order parameter that distinguishes between the bilayer sheet and square grid

structures. The general procedure for calculating the order parameter is as follows. First, we choose the final self-assembled structures as reference states. Second, we extract a pattern representative of each reference state by choosing a suitable length scale. The cutoff window of interest is chosen to be [4.0σ, 5.0σ] to capture the distance between the rods belonging to parallel bilayer ribbons in both structures. The bond order diagrams of the reference structures (Figure 6) show that within that cutoff window the extracted patterns of the reference columnar square grid structure and bilayer sheets are clearly distinguishable. Subsequently, the Fourier shape descriptor of the extracted patterns of the reference states is determined. Similarly, the Fourier shape descriptor of subsequent snapshots during self-assembly and transformation is determined and compared with that of the reference states. The matching between the shape descriptors is used as the order parameter: the closer the order parameter is to unity, the more the structure approaches the reference state. As shown in Figure 7, the evolution of the system toward the target structures in the self-assembly process from isotropic states is compared with that in the counterpart transformation process at $T = 1.4\varepsilon/k_B$. The snapshots at different times in the right column show that *the transformed systems approach the target states faster than self-assembly from isotropic states* (Figure 8). This is presumably because of the presence of aligned rod bilayer ribbons in both ordered configurations, as indicated by the sharp first and second peaks of $g_{R-R}(r)$. While it takes self-assembly processes a certain amount of time to form these ribbons starting from isotropic states, the transformation processes proceed from the ribbons immediately after the rods change length. Thus for these particular ordered states, and for this particular building block, for which there is a common substructure within both target structures (the ribbons), transformation is more efficient than assembly from a disordered state. For transformations between other ordered states that share no common substructures, whether self-assembly or reconfiguration is faster is an open and interesting question to be pursued in subsequent work. In the present system, the time scale of the transformation process is within 20 million steps, which we estimate is equivalent to several microseconds of real time considering actual nanoparticle and polymer tether interactions.

CONCLUSION

While reconfigurability can easily be found in biological systems and certain liquid crystals, few examples are available for traditional synthetic materials, especially those based on nanoparticles. In this work, the reconfigurability between bilayer sheets and square grid structures assembled by laterally tethered nanorods serves to inspire the fabrication of next generation nanomaterials able to reconfigure in response to a dy-
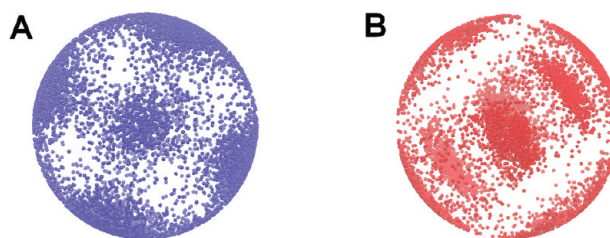
Figure 6. Bond order diagram of (A) the square grid structure and (B) bilayer sheets within the cutoff range of [4.0σ, 5.0σ].

namic change in the building block shape. Additionally, the emergence of honeycomb and pentagonal grid structures at intermediate rod lengths implies that all reported structures can be reversibly transformed one to another by tuning the rod length on the fly. We envision that the ordered periodic structures we obtain can be useful for a range of problems. For example, optical materials with a photonic band gap or negative index of refraction require particular symmetries or structures.[15,20] By switching between a 2-D (sheets) to 3-D (square grid) structure with 1-D and 2-D periodicity, respectively, where the rods are composed of a high dielectric material, it may be possible to turn on and off interesting nonlinear optical properties. The cavities provided by the square grid structure with the tethers removed post-assembly might also be useful for waveguide applications. Alternatively, the mechanical properties of a layered sheet *versus* 3-D grid structure should be very different, and thus reconfigurable rods assembled into these structures could be used to fabricate a material that, for example, flows or is stable under a small shear. The kinetic effects due to rod lengthening/shortening are shown not to obstruct the
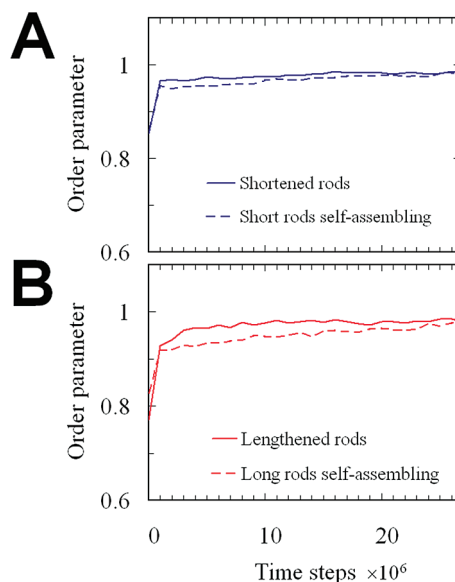
Figure 7. Comparison of (A) self-assembly of short rods from disordered states and order−order transformation induced by shortening rods; and (B) self-assembly of long rods from disordered states and order−order transformation induced by lengthening rods.

A

Shortened rods   Short rods self-assembling

t = 0

t = 10×10⁶

t = 20×10⁶

B   Lengthened rods   Long rods self-assembling

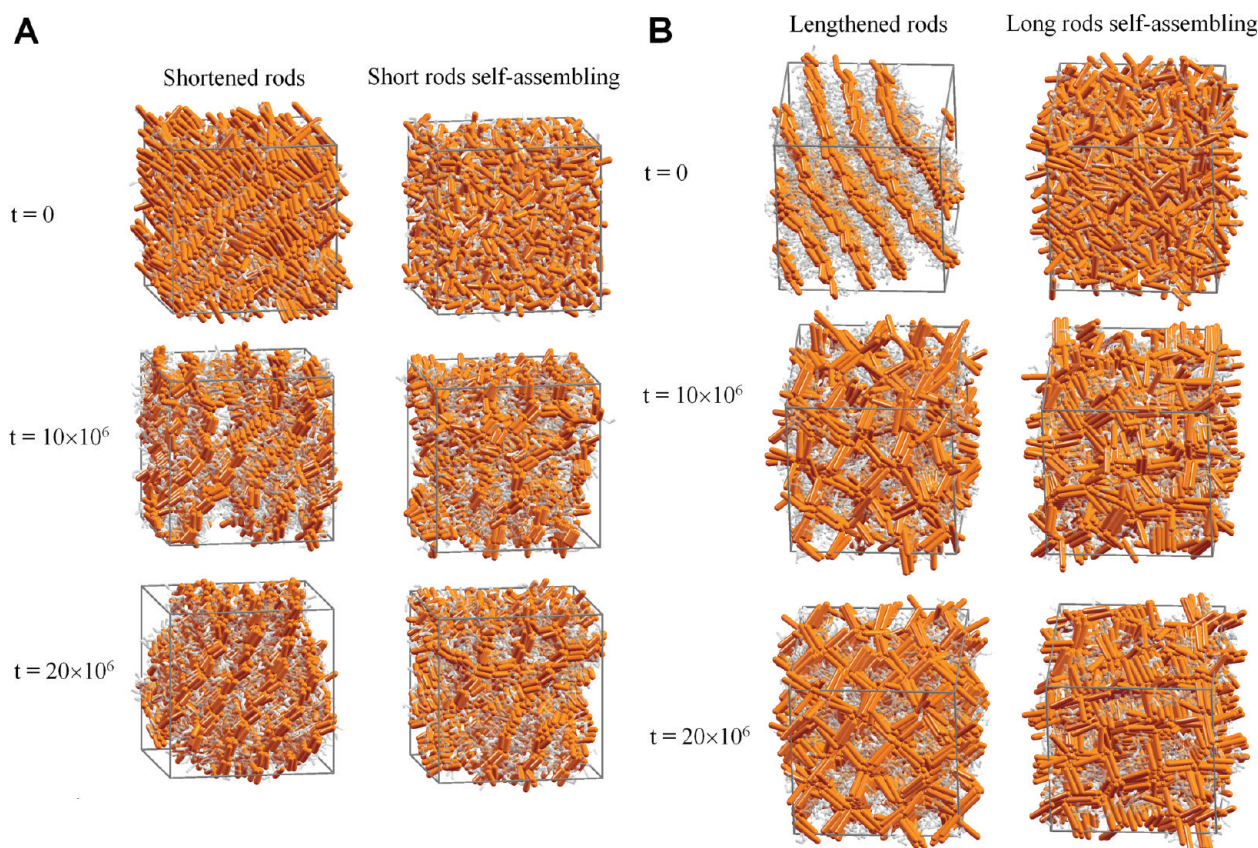

t = 0

t = 10×10⁶

t = 20×10⁶

Figure 8. (A) System snapshots corresponding to the time slices on the order parameter plot in Figure 7A. (B) System snapshots corresponding to the time slices on the order parameter plot in Figure 7B.

evolution of the system toward equilibrium, but instead expedite the formation of the target structures over the self-assembly process from disordered states. Although the experimental viability of a reversible rod shortening and lengthening procedure has not yet been demonstrated in the literature, we envision that such shape-shifting can be controlled at nanometer scales through the use of, for example, anisotropic cross-linking within an organic rod made of a polymer gel, or in a similar manner to tuning the conformation of polypeptide-based building blocks[36−39] or melting nanorods using femtosecond or nanosecond laser pulses.[43−45] Despite the simple shape change considered here, the approach is applicable to more interesting shape changes that involve changes in symmetry and/or topology.

METHODS

Simulation Model. We use a minimal model of laterally tethered nanorods similar to one used in our previous work[11−13] that captures the essential physics of the studied systems (Figure 1) including the geometry of the rods and the flexibility of the laterally attached tethers. The center bead of a rod is linked with the tether *via* a finitely extensible nonlinear elastic (FENE) spring. The tethers are modeled as linear chains of three spherical beads with diameter σ, bonded *via* FENE springs. We utilize empirical potentials[24] that are successful in capturing the relevant physics of rod−coil molecules, block copolymers, and surfactants.[48] To model the aggregation of the rods and that of the tethers, the interactions between the rod beads and between the tether beads are modeled by the 12−6 Lennard-Jones potential truncated and shifted to zero at the cutoff distance of 2.5σ to incorporate short-range attraction and excluded volume interactions. Immiscible species tend to segregate; therefore, the rod−tether interaction is modeled by the softly repulsive Weeks−Chandler−Andersen (WCA) potential to capture their immiscibility. In our simulations, the potential energy well depths, ε, are chosen to be identical for rod−rod, tether−tether, and rod−tether interactions: $\varepsilon_{R-R} = \varepsilon_{T-T} = \varepsilon_{R-T}$

$= \varepsilon$. The natural units for these systems are the bead diameter, σ, the bead mass, m, and ε. The time scale is accordingly defined as $\tau = \sigma(m/\varepsilon)^{1/2}$. For block copolymer and nanoparticle systems, typical values of these parameters are $\sigma = 5$ nm, $m = 10^{-21}$ kg, $\varepsilon = 50$ kJ/mol, and $\tau = 0.5$ ns.

Simulation Method. Brownian dynamics (BD) is used to simulate the self-assembly of tethered nanorods in a melt-like condition in three dimensions. In BD, the random and drag forces in the equation of motion for each bead serve as a momentum nonconserving thermostat for the system, and our simulations sample the *NVT* ensemble, where N is the total number of beads, V is the box volume, and T is temperature. Details of this method can be found elsewhere.[26] The friction coefficient γ is set to be 1.0 to limit the ballistic motion of a bead in a time step to be less than 1.0σ. The rotational degrees of freedom of the rods are incorporated using the equations for rotation of rigid bodies with quaternions. We employ the velocity Verlet scheme to integrate the equation of motion of the tether beads and to advance the rotational motion of the rod pairs with a time step $\Delta t = 0.002\tau$. For self-assembly simulations, we use a similar procedure to that used in our previous phase diagram mapping simulations[11,25,31,32] to sample the system at a number density of $N/V = 0.8$, which

is sufficiently high to reproduce a melt-like condition. We cool the system from an initial temperature of $T = 2.5\varepsilon/k_B$, corresponding to a disordered state, by decreasing T step-by-step with $\Delta T = 0.1\varepsilon/k_B$. At each temperature step, we equilibrate the system until we observe fluctuations in the system potential energy U of less than 5% and a morphology that does not substantially change over a time scale of $\sim$20 million time steps. A typical simulation run requires $50-100$ million time steps, equivalent to microseconds in real time for a typical experimental system. We also heat and cool the systems with different schedules to ascertain that the cooling paths do not bias the assembled structures. By following this procedure, we seek to find equilibrium assembled structures and obtain a consistent estimate of the disorder−order temperature for our particular systems. Once the assembled structures are stabilized at temperatures lower than the disorder−order transition, we perform the rod shortening or lengthening by sliding the rod beads along the rod director while maintaining the rod center of mass. To simplify our shape-changing procedure in the present study, we assume that (1) the rod shortening/lengthening rate is uniform for all building blocks, (2) the building block symmetry is conserved, and (3) the interactions between rods are fixed during shortening and lengthening. The rods are shortened or lengthened every 10 time steps until the target length is reached. We use different shape-changing rates of $2 \times 10^{-2}\sigma$, $2 \times 10^{-3}\sigma$, 2×10^{-4}, and $2 \times 10^{-5}\sigma$ every 10 time steps to ascertain whether any kinetic effects due to rod lengthening/shortening influence the transformation processes. For example, a rate of $2 \times 10^{-3}\sigma$ every 10 time steps means that the rods obtain the target length after 10 000 simulation steps, equivalent to approximately 10 ns in real time. We note that these transformation rates are sufficiently small that overlaps do not occur during rod lengthening in the temperature range studied ($T \leq 2.5\varepsilon/k_B$) with the chosen integration time step $\Delta t = 0.002\tau$. To ensure that finite size effects are avoided with regards to assembled structures and disorder−order temperature, we run test simulations on several system sizes of $N_B = 500$, 1000, and 2000 building blocks, corresponding to $N = 4000$, 8000, and 16 000 beads, respectively. For each system size, we also run simulations with different random number sequences for the thermostat and initial configuration and initial velocity profiles to avoid any artifacts of the random number generator. During the simulation, the number of beads (N), box volume (V), and interaction strengths (ε) between species are held fixed. We choose to show the data for $N_B = 2000$ and the rod lengthening/shortening rate of $2 \times 10^{-3}\sigma$ every 10 time steps as our representative results in the main text. Our simulations are conducted using LAMMPS, an open source parallel molecular dynamics code,[49] with a LAMMPS extension we developed for this work that allows three-dimensional rigid bodies to change their geometry during simulations.

Supporting Information Available: Simulation results for different rod lengths and system sizes. This material is available free of charge *via* the Internet at http://pubs.acs.org.

REFERENCES AND NOTES

1. Guo, Y.; Ma, Y.; Xu, L.; Li, J.; Yang, W. Conformational Change Induced Reversible Assembly/Disassembly of Poly-L-Lysine-Functionalized Gold Nanoparticles. *J. Phys. Chem. C* **2007**, *111*, 9172–9176.
2. Thisayukta, J.; Takezoe, H.; Watanabe, J. Study on Helical Structure of the B4 Phase Formed from Achiral Banana-Shaped Molecule. *Jpn. J. Appl. Phys.* **2001**, *40*, 3277–3287.
3. Shao, H.; Parquette, J. R. Controllable Peptide-Dendron Self-Assembly: Interconversion of Nanotubes and Fibrillar Nanostructures. *Angew. Chem., Int. Ed.* **2009**, *48*, 2525–2528.
4. Reddy, R. A.; Tschierske, C. Bent-Core Liquid Crystals: Polar Order, Superstructural Chirality and Spontaneous Desymmetrisation in Soft Matter Systems. *J. Mater. Chem.* **2006**, *16*, 907–961.
5. Lim, Y.; Moon, K.-S.; Lee, M. Recent Advances in Functional Supramolecular Nanostructures Assembled from Bioactive Building Blocks. *Chem. Soc. Rev.* **2009**, *38*, 925–934.
6. Sun, A.; Lahann, J. Dynamically Switchable Biointerfaces. *Soft Matter* **2009**, *5*, 1555–1561.
7. Kim, J.-K.; Lee, E.; Lim, Y.-B.; Lee, M. Supramolecular Capsules with Gated Pores from an Amphiphilic Rod Assembly. *Angew. Chem., Int. Ed.* **2008**, *47*, 4662–4666.
8. Fernyhough, C.; Ryan, A. J.; Battaglia, G. Ph Controlled Assembly of a Polybutadiene-Poly(methacrylic acid) Copolymer in Water: Packing Considerations and Kinetic Limitations. *Soft Matter* **2009**, *5*, 1674–1682.
9. Lee, E.; Kim, J.-K.; Lee, M. Reversible Scrolling of Two-Dimensional Sheets from the Self-Assembly of Laterally Grafted Amphiphilic Rods. *Angew. Chem., Int. Ed.* **2009**, *48*, 3657–3660.
10. Ciszek, J. W.; Huang, L.; Wang, Y.; Mirkin, C. A. Kinetically Controlled, Shape-Directed Assembly of Nanorods. *Small* **2008**, *4*, 206–210.
11. Horsch, M. A.; Zhang, Z.; Glotzer, S. C. Self-Assembly of Laterally-Tethered Nanorods. *Nano Lett.* **2006**, *6*, 2406–2413.
12. Hong, D.-J.; Lee, E.; Jeong, H.; Lee, J.; Zin, W.-C.; Nguyen, T. D.; Glotzer, S. C.; Lee, M. Solid-State Scrolls from Hierarchical Self-Assembly of T-Shaped Rod−Coil Molecules. *Angew. Chem., Int. Ed.* **2009**, *48*, 1664–1668.
13. Nguyen, T. D.; Glotzer, S. C. Switchable Helical Structures Formed by the Hierarchical Self-Assembly of Laterally-Tethered Nanorods. *Small* **2009**, *5*, 2092–2096.
14. Ryu, J.-H.; Hong, D.-J.; Lee, M. Aqueous Self-Assembly of Aromatic Rod Building Blocks. *Chem. Commun.* **2008**, *9*, 1043–1054.
15. Ryu, J.-H.; Lee, M. Liquid Crystalline Assembly of Rod−Coil Molecules. *Struct. Bonding (Berlin)* **2008**, *128*, 63–98.
16. Zhou, Q.; Chen, T.; Zhang, J.; Wana, L.; Xie, P.; Han, C. C.; Yan, S.; Zhang, R. Hierarchical Self-Assembly of *p*-Terphenyl Derivative with Dumbbell-like Amphiphilic and Rod−Coil Characteristics. *Tetrahedron Lett.* **2008**, *49*, 5522–5526.
17. Kieffer, R.; Prehm, M.; Pelz, K.; Baumeister, U.; Liu, F.; Hahn, H.; Lang, H.; Ungar, G.; Tschierske, C. Siloxanes and Carbosilanes as New Building Blocks for T-Shaped Bolaamphiphilic LC Molecules. *Soft Matter* **2009**, *5*, 1214–1227.
18. Crane, A. J.; Martínez-Veracoechea, F. J.; Escobedo, F. A.; Müller, E. A. Molecular Dynamics Simulation of the Mesophase Behaviour of a Model Bolaamphiphilic Liquid Crystal with a Lateral Flexible Chain. *Soft Matter* **2008**, *4*, 1820–1829.
19. Lee, E.; Huang, Z.; Ryu, J.-H.; Lee, M. Rigid-Flexible Block Molecules Based on a Laterally Extended Aromatic Segment: Hierarchical Assembly into Single Fibers, Flat Ribbons, and Twisted Ribbons. *Chem.—Eur. J.* **2008**, *14*, 6957–6966.
20. Tschierske, C. Liquid Crystal Engineering—New Complex Mesophase Structures and Their Relations to Polymer Morphologies, Nanoscale Patterning and Crystal Engineering. *Chem. Soc. Rev.* **2007**, *36*, 1930–1970.
21. Israelachvili, J. N. *Intermolecular and Surface Forces*; Academic: London, 1992.
22. Bates, F. S.; Fredrickson, G. H. Block Copolymer Thermodynamics: Theory and Experiment. *Annu. Rev. Phys. Chem.* **1990**, *41*, 525–527.
23. Schultz, A. J.; Hall, C. K.; Genzer, J. Computer Simulation of Copolymer Phase Behavior. *J. Chem. Phys.* **2002**, *117*, 10329–10338.

24. Zhang, Z.; Glotzer, S. C. Tethered Nano Building Blocks: Toward a Conceptual Framework for Nanoparticle Self-Assembly. *Nano Lett.* **2003**, *3*, 1341–1346.

25. Horsch, M. A.; Zhang, Z.; Glotzer, S. C. Self-Assembly of Polymer-Tethered Nanorods. *Phys. Rev. Lett.* **2005**, *95*, 056105-4.

26. Iacovella, C. R.; Horsch, M. A.; Zhang, Z.; Glotzer, S. C. Phase Diagrams of Self-Assembled Mono-Tethered Nanospheres from Molecular Simulation and Comparison to Surfactants. *Langmuir* **2005**, *21*, 9488–9494.

27. Zhang, X.; Chan, E. R.; Glotzer, S. C. Self-Assembled Morphologies of Monotethered Polyhedral Oligomeric Silsesquioxane Nanocubes from Computer Simulation. *J. Chem. Phys.* **2005**, *123*, 184718-6.

28. Chan, E. R.; Zhang, X.; Lee, C. Y.; Neurock, M.; Glotzer, S. C. Simulations of Tetra-Tethered Organic/Inorganic Nanocube-Polymer Assemblies. *Macromolecules* **2005**, *38*, 6168–6180.

29. Horsch, M. A.; Zhang, Z.; Glotzer, S. C. Simulation Studies of Self-Assembly of End-Tethered Nanorods in Solution and Role of Rod Aspect Ratio and Tether Length. *J. Chem. Phys.* **2006**, *125*, 184903–184912.

30. Zhang, X.; Zhang, Z.; Glotzer, S. C. Simulation Study of Cyclic-Tethered Nanocube Self-Assemblies: Effect of Tethered Nanocube Architectures. *Nanotechnology* **2007**, *18*, 115706-6.

31. Iacovella, C. R.; Glotzer, S. C. Complex Crystal Structures Formed by the Self-Assembly of Ditethered Nanospheres. *Nano Lett.* **2009**, *9*, 1206–1211.

32. Nguyen, T. D.; Zhang, Z.; Glotzer, S. C. Molecular Simulation Study of Self-Assembly of Tethered V-Shaped Nanoparticles. *J. Chem. Phys.* **2008**, *129*, 244903–244911.

33. Iacovella, C. R.; Glotzer, S. C. Phase Behavior of Ditethered Nanospheres. *Soft Matter* **2009**, *5*, 4492–4498.

34. Horsch, M. A.; Zhang, Z.; Glotzer, S. C. Self-Assembly of End-Tethered Nanorods in a Neat System and Role of Block Fractions and Aspect Ratio. *Soft Matter* **2010**, *6*, 945–954.

35. Jayaraman, A.; Schweizer, K. S. Structure and Assembly of Dense Solutions and Melts of Single Tethered Nanoparticles. *J. Chem. Phys.* **2008**, *128*, 164904–164913.

36. Chockalingam, K.; Blenner, M.; Banta, S. Design and Application of Stimulus-Responsive Peptide Systems. *Protein Eng.* **2007**, *20*, 155–161.

37. Lin, J.; Zhu, G.; Zhu, X.; Lin, S.; Nose, T.; Ding, W. Aggregate Structure Change Induced by Intramolecular Helix-Coil Transition. *Polymer* **2008**, *49*, 1132–1136.

38. Gebhardt, K. E.; Ahn, S.; Venkatachalam, G.; Savin, D. A. Rod−Sphere Transition in Polybutadiene-Poly(L-Lysine) Block Copolymer Assemblies. *Langmuir* **2007**, *23*, 2851–2856.

39. Gebhardt, K. E.; Ahn, S.; Venkatachalam, G.; Savin, D. A. Role of Secondary Structure Changes on the Morphology of Polypeptide-Based Block Copolymer Vesicles. *J. Colloid Interface Sci.* **2008**, *317*, 70–76.

40. Ahmed, Z.; Myshakina, N. S.; Asher, S. A. Dependence of the AmII′P Proline Raman Band on Peptide Conformation. *J. Phys. Chem. B* **2009**, *113*, 11252–11259.

41. Sebba, D. S.; Mock, J. J.; Smith, D. R.; LaBean, T. H.; Lazarides, A. A. Reconfigurable Core-Satellite Nanoassemblies as Molecularly-Driven Plasmonic Switches. *Nano Lett.* **2008**, *8*, 1803–1808.

42. Maye, M. M.; Kumara, M. T.; Nykypanchuk, D.; Sherman, W. B.; Gang, O. Switching Binary States of Nanoparticle Superlattices and Dimer Clusters by DNA Strands. *Nat. Nanotechnol.* **2010**, *5*, 116–120.

43. Chang, S.-S.; Shih, C.-W.; Chen, C.-D.; Lai, W.-C.; Wang, C. R. C. The Shape Transition of Gold Nanorods. *Langmuir* **1999**, *15*, 701–709.

44. Link, S.; Wang, Z. L.; El-sayed, M. A. How Does a Gold Nanorod Melt? *J. Phys. Chem. B* **2000**, *104*, 7867–7870.

45. Link, S.; Burda, C.; Nikoobakht, B.; El-sayed, M. A. Laser-Induced Shape Changes of Colloidal Gold Nanorods Using Femtosecond and Nanosecond Laser Pulses. *J. Phys. Chem. B* **2000**, *104*, 6152–6163.

46. Glotzer, S. C.; Solomon, M. J. Anisotropy of Building Blocks and Their Assembly into Complex Structures. *Nat. Mater.* **2007**, *6*, 557–562.

47. Keys A. S.; Iacovella C. R.; Glotzer, S. C. Creating Flexible Order Parameters Using Shape Matching and Applications to Assembly. Preprint.

48. Larson, R. G. *The Structure and Rheology of Complex Fluids*; Oxford University Press: New York, 1999.

49. Plimpton, S. J. Fast Parallel Algorithms for Short-Range Molecular Dynamics. *J. Comput. Phys.* **1995**, *117*, 1–19.